
SYNTHESIS AND STRUCTURAL STUDIES ON CO^{II}-Y AND A UNIQUE CO^{II}(HYDRAZONE)/Y ZEOLITES USING THEM AS EFFICIENT ALTERNATIVES FOR NOBLE METAL CATALYSTS

AYMAN H. AHMED

Department of Chemistry, Faculty of Science, Al-Azhar University, Nasr City, Cairo, Egypt.

Abstract

Co^{II}(SBSH)/Y has been prepared by solid-solid interaction of Co^{II}-Y with salicylidinebenzenesulphonylhydrazone ligand using the flexible ligand method and its activity toward CO oxidation was examined and compared with Co^{II}-Y. The composition and structure of this new catalyst have been identified. The prepared zeolites have been characterized by elemental analysis, FTIR, UV-Vis., magnetic measurements, XRD and thermal (TG, DTA) as well as surface area measurements and nitrogen adsorption studies. The results showed that the Co(II) ions in zeolite-Y are coordinated with the ligand through the (C=N), (NH), (SO₂) and (OH) groups with replacing of one proton from the latter group forming 3:1 metal - ligand encapsulated complex differs completely from that prepared in solution. The resulting catalyst was found to be thermally stable up to 1000 °C. Adsorption of CO at room temperature on Co^{II}-Y and Co^{II}(SBSH)/Y showed peaks characteristic to CO₂ (as an oxidation product) and different Co-carbonyl species which indicated the presence of different oxidation states of cobalt. The FTIR spectra indicated the presence of carboxyl group and different carboxylate species after CO adsorption at room temperature (RT). It is concluded that, the oxidation of CO on Coⁿ⁺ (n ≤ 2) sites is already starting at room temperature and hence it may be considered as an efficient alternative for noble metal catalysts used in the CO oxidation reaction.

Keywords: Zeolite encapsulated Co^{II}-hydrazone complexes; FL method

Introduction

In spite of lot of knowledge has been acquired regarding to heterogeneous catalysis, there is need to find efficient and ecofriendly catalyst system which would operate under mild conditions. Various attempts for the development of new catalyst system led to the emergence of a new class of catalyst called “ zeolite encapsulated metal complexes “ (ZEMC).

There were basically three approaches to the preparation of these ship-in-a-bottle chelate complexes, namely the flexible ligand method, the template synthesis

method and the zeolite synthesis method. In the first approach, a flexible ligand must be able to diffuse freely through the zeolite pores but upon complexation with a previously exchanged metal ion, the complex becomes too large and rigid to escape the cage⁽¹⁻⁴⁾. The template synthesis method is exemplified by the preparation of intrazeolite metallophthalocynines⁽⁵⁻⁷⁾ where the diffused four dicyanobenzene (DCB) into the zeolite pores can cyclize around a resident metal ion to form a complex which is too large to exit. The third approach referred to as the zeolite synthesis method which is the newest method for encapsulating metal complexes in zeolites where the metal complex is added, possibly in a template role, during the crystallization of the zeolite host^(8,9).

Generally, the intrazeolite complexes have been characterized by different techniques including FTIR, UV-Vis., Raman, ESR, NMR, Mossbauer and XPS spectroscopy as well as X-ray diffraction and microscopy. Additionally, surface area measurements, adsorption studies and thermal analysis have provided an evidence for the intrazeolite location of the metal complexes. A number of encapsulated metal complexes have been reported in^(10,11) and these catalysts under ideal conditions can mimic certain enzymes^(2, 12-15). Although large number of encapsulated Co (II) complexes have been studied and prepared using different classes of ligand e.g. phthalocyanines⁽¹⁶⁾, schiff bases^(2,11,17-19) poly (pyridines)^(20,21), oxime⁽²²⁾, alkanes⁽²³⁾ and some amines⁽²⁴⁾, the hydrazones did not use till now with the exchanged Co (II) ions. In fact, investigation of the interactions between transition metals surfaces and different adsorbed substances has been the focus of intensive studies for many years due to their potential use as catalysts⁽²⁵⁾. Following the classification of many authors⁽²⁶⁻²⁸⁾, cobalt is a border-line element which, under particular conditions, can dissociate CO. Improving the efficiency of CO adsorption and oxidation over Co^{II}-Y may be done by encapsulating organometallic complexes in zeolites. In this study, CO will be admitted on Co^{II}-Y and Co^{II}(SBSH)/Y and the adsorption results will be traced by in-situ FTIR spectroscopy.

The aim of the present paper is to encapsulate the Co (II) hydrazone complex in the Y zeolite by a flexible ligand method and investigate the CO oxidation for this new material compared with Co^{II}-Y. The compositions and structures of cobalt exchanged Y and the encaged complex have been reported and the texture of these zeolites are described to confirm the immobilization of the complex inside the zeolite matrix as well as showing the capability of using these composites as heterogeneous catalysts.

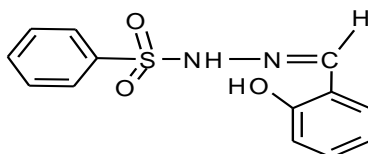
Experimental

Materials

All the reagents and solvents used for the preparation of the ligand and modified zeolites were of Aldrich or Analar grade quality. The zeolite host material was NaY (lot. no. D1-9915, HSZ- 320N – NAA and Si/Al = 5.6).

Preparation of ligand, SBSH.

The hydrazone ligand (L) with the chemical formula $\text{C}_{13}\text{H}_{12}\text{N}_2\text{O}_3\text{S}$, used under investigation is salicylidinebenzenesulphonylhydrazone (SBSH), and has the structural formula shown in Fig. 1. It was prepared using the procedure described in the literature⁽²⁹⁾ but with little modification. Where an EtOH solution of benzenesulphonylhydrazine was refluxed for 4 h with EtOH solution of salicylaldehyde (1:1) in the presence of 2 - 3 drops glacial acetic acid. On cooling, white crystals of SBSH formed were washed with ethanol, recrystallized from hot EtOH and finally dried at 80°C for 2 h in furnace (m.p.=155, lit. m.p.=155 $^\circ\text{C}$).



(SBSH)

Fig. 1.

Preparation of metal- exchanged zeolite-Y, $\text{Co}^{\text{II}}\text{-Y}$.

7.0 g NaY zeolite was treated at room temperature with 1500 ml of 0.01 M acetate solution of Co (II), the pH of the resulting mixture was in the pH 5 - 6 range. The ion exchange was conducted for 48 h with continuous stirring. The solid was filtered off, washed thoroughly with distilled water till the washing solution was free from any cobalt ion content. The zeolite was then dried in air at room temperature for 12 h and finally stored over saturated ammonium chloride solution until required for use.

Preparation of zeolite encapsulated cationic cobalt complex, $\text{Co}^{\text{II}}(\text{SBSH})/\text{Y}$.

This new material was prepared by solid - solid interaction method as follow. 1.0 g of $\text{Co}^{\text{II}}\text{-Y}$ prepared earlier was dehydrated under vacuum (10^{-4} Torr) in Pyrex shrink tube at 200°C for 2 h. After cooling, $\text{Co}^{\text{II}}\text{-Y}$ was intimately mixed in inert-atmosphere glove bag with excess of SBSH ligand. The resultant mixture was placed

horizontally in a shrink furnace tube, evacuated again to 10^{-4} Torr for 10 min and then heated for 4 h at 135°C . The tube was allowed to cool to room temperature, opened carefully and the product was washed several times with successive portions of hot solvents (ethanol, acetone and methylene chloride) followed by Soxhlet-extraction with ethanol for 48 h in normal conditions to remove the excess of ligand. Finally, the sample was dried at 80°C in oven for 8 h.

Physical measurements

The metal content (M %) was determined by complexometric titration with EDTA using xylenol orange indicator, hexamine buffer and sodium fluoride as a masking agent for the interfering aluminium ions result from disintegration of the zeolite framework⁽³⁰⁾. The results obtained were confirmed by using Varian atomic absorption spectrometer (Varian-AA220). The carbon was determined by Microanalyses at Cairo University, Egypt. X-ray powder diffraction (XRD) patterns were recorded on PW1840 Philips diffractometer using $\text{Cu } \alpha$ radiation ($\lambda=1.54 \text{ \AA}$) and the UV-Vis. spectra of the samples were recorded in Nujol scanning the range 200 - 1100 nm using lambda 35 Perkin- Elmer UV-Vis. spectrophotometer. Infrared spectra of solid samples (KBr pellets) were recorded on a Mattson 5000 FTIR spectrometer through the range 200 - 4000 cm^{-1} . The mass susceptibility of the solid materials was measured at room temperature using magnetic susceptibility balance of Johnson Metthey Sherwood models. TG, DTG and DTA were measured on a Shimadzu 50 H thermal analyzer. In-situ infrared (IR) spectra were recorded with FTIR instrument Bruker (Vector 22) single beam spectrometer at a spectral resolution of 2.0 cm^{-1} . Self-supporting discs, made by pressing 30 mg of powder to a pressure of 5 tons, were placed in an IR cell connected to a high vacuum system in which a pressure of 10^{-4} Torr could be maintained. 50 Torr of CO was admitted on the samples at room temperature (RT) after being thermally evacuated for 1 h at 200°C . The cell was allowed to equilibrate for 20 min and, then evacuated at room temperature and 50°C . At each step, the FTIR spectrum was recorded after cooling down to room temperature.

Results and discussion

FTIR spectroscopy

IR spectroscopy can provide information on the encapsulated metal complexes and on the crystallinity of the host zeolite. FTIR spectra of NaY and of the modified zeolites ($\text{Co}^{\text{II}}\text{-Y}$, $\text{Co}^{\text{II}}(\text{SBSH})/\text{Y}$) are dominated by the Y zeolite bands assignable to

surface hydroxylic group, internal and external vibrations. The sample is still retaining its crystallinity as obtained from IR spectra and confirmed from XRD. There is no any significant change in a shape or position of the zeolite structure-sensitive bands (1137, 790, 384, 580 cm⁻¹) associated with the dealumination and/or the distortion. This foundation manifested the absence of any interaction between the exchanged metal cations and the framework structure ruling out the probability of sharing the oxygen of the zeolite lattice in coordination. The new band observed at 1400 cm⁻¹ in the infrared spectra of modified samples (Co^{II}-Y, Co^{II}(SBSH)/Y) is mainly due to δ OH (in plane) of coordinated H₂O with the metal ions⁽³¹⁾. Studding the IR spectra of Co^{II}(SBSH)/Y within the 1200 - 1600 cm⁻¹ region (in which the Y zeolite has not been absorbed) with that of the free ligand (SBSH) reported in literature⁽²⁹⁾ reveals the following facts (1) $\nu_{as}(\text{SO}_2)$ of the ligand is shifted to higher upon complexation and appeared at 1348 cm⁻¹ suggesting the involvement of this group in coordination. The absence of splitting of this group emphasize the presence of one type of (S=O) group. (2) $\delta(\text{NH})$ is remained at the same position without any shift indicating that this group did not take part in coordination. (3) $\delta(\text{OH})$ observed in the ligand disappeared upon encapsulation showing the deprotonation and thus participation of this group in coordination. (4) $\nu(\text{C}=\text{N})$ is most probably shift to lower upon complexation and overlaped with the band assigned to the adsorbed water (observed in between 1720-1570 cm⁻¹) suggesting the involvement of this group in coordination. Furthermore, the appearance of other additional weak bands at 1450, 1475 and 1570 cm⁻¹ may be due to $\nu(\text{C}=\text{C})$ of the phenyl ring.

Table 1. Chemical composition, physical and analytical data for SBSH and the prepared zeolites.

Sample label	Colour	M%	M.p °C	M/C ratio Found (calcd.)	χ_g c.g.s.	Product assignment
SBSH	White	-	155	-	-	-
NaY	White	-	> 300	-	diamag	-
Co ^{II} -Y	Pale pink	5.90	> 300	-	1.044×10^{-5}	[Co(H ₂ O) ₆] ²⁺ -Y
Co ^{II} (SBSH)/Y	Yellow	5.64	> 300	0.3222 (0.231)	0.798×10^{-5}	[Co ₃ (SBSH)(H ₂ O) ₁₄] ⁵⁺ -Y

Electronic spectra and magnetic properties

The pale pink sample of the formula Co^{II}-Y shows four absorption bands at 26595 cm⁻¹, 25000 cm⁻¹, 20000 cm⁻¹ and 14285 cm⁻¹. The first two bands are mainly due to charge - transfer in zeolite Y – support while the latter two bands are

probably assigned to ${}^4T_{1g} \rightarrow {}^4T_{1g} (p)$ and ${}^4T_{1g} \rightarrow {}^4A_{2g}$ transitions, in an octahedral geometry around the Co (II) ion^(32,33). The paramagnetic value of χ_g supports that the Co^{II} ion is octahedrally coordinated.

The electronic spectrum of encapsulated Co (II) complex exhibits two bands at 25773 cm^{-1} and 19608 cm^{-1} assigned to M \rightarrow L charge – transfer and ${}^4T_{1g} \rightarrow {}^4T_{1g} (P)$ transition, in an octahedral configuration^(32,33) around the Co (II) ion. The paramagnetic value of χ_g is consistent with an octahedral geometry around the Co (II) ion.

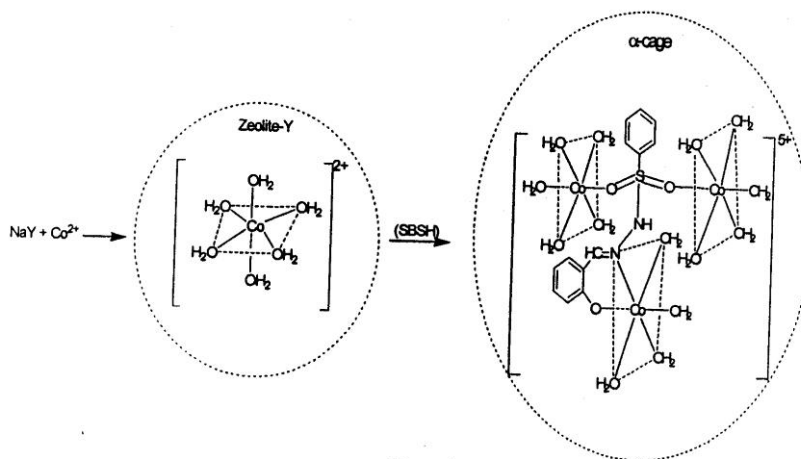
Based on the foregoing results of elemental analysis, (IR, UV-Vis.) spectra and the magnetism (Table 1) for the zeolite samples under investigation, the flexible ligand synthesis showing the spatial configuration of the ligated groups around the central metal ion inside Y zeolite can be represented by scheme 1.

X-Ray diffraction

XRD showed that the crystallinity and morphology of NaY zeolite is almost retained intact in spite of the occlusion of the Co (II) ions and its complex in it (Fig 2) and This result is in good agreement with IR results obtained previously. The diffractograms did not show any lines refer to the presence of any new phase. Further, the changed observed in the relative intensities of the 311, 220 reflections upon introducing the metal ions or its related complex result from that reported⁽³⁴⁾ where the exchanging of large cations in zeolite Y leads to disturb the random distribution of small extra framework cations (Na^+). This change in location of small cations affects the relative intensities of 311, 220 peaks. Analysis of patterns in Fig. 2. clearly shows this trend where the introducing of exchanged metal cations or their corresponding complexes result in a significant cation redistribution. This of course indicates that the entrapped large complex displaced sodium ions from their random positions in the supercages to locations at sites II, I $\bar{6}$ and are placed inside the cages of zeolite Y .

Thermal analysis

The TG curve of NaY shows four stages of weight loss in the 30 - 1000 °C range starting at 46, 101, 187 and 503 °C corresponding to the water loss from surface, wide and narrow pores of Y zeolite. The appearance of two endothermic peaks at 717 and 742 °C in DTA curve suggests some sort of physical changes such as the change of crystal morphology or phase transitions.



The thermogram (TG) of the $\text{Co}^{\text{II}}\text{-Y}$ sample showed three endothermic peaks at 81, 141, and 268°C corresponding to the loss of water from the pores inside the zeolite. The peak observed at 531°C reflects the decomposition. The DTA curve showed one exothermic peak at 535 and an endothermic one at 960°C. The first peak was accompanied by weight loss due to a decomposition process, while the second peak at 906°C was not accompanied by weight loss assignable to a phase changes such as the change of crystal morphology or physical transition.

The TG thermogram of $\text{Co}^{\text{II}}(\text{SBSH})/\text{Y}$ showed two stages of decomposition starting at 39 and 566°C corresponding to the removal of adsorbed water from the zeolite. On the other hand, the DTA pattern showed only one endothermic peak at 50°C accompanied by weight loss indicating the desorption of water. The absence of any exothermic weight loss peak assigned to the decomposition of the encapsulated complex in the 30 - 1000°C region (in DTA) suggests the stability of that complex through this range of temperatures.

Surface studies

The BET-surface areas (S_{BET}) of NaY, $\text{Co}^{\text{II}}\text{-Y}$ and $\text{Co}^{\text{II}}(\text{SBSH})$ were determined from nitrogen adsorption isotherms measured at -196°C. The obtained isotherms of NaY and $\text{Co}^{\text{II}}\text{-Y}$ are belong to type II of Brunauer's classification⁽³⁵⁾ with hysteresis loops at relative vapour pressure P/P^0 of 0.15 - 0.95. It was seen from the V_{1-t} plots that, NaY zeolite is characterized by the domination of narrow pores while its metal exchanged ($\text{Co}^{\text{II}}\text{-Y}$) acquire wide porosity. This indicates the creation of new type of pores structures after exchange with the metal ions in zeolite⁽³⁶⁾. In case of $\text{Co}^{\text{II}}(\text{SBSH})/\text{Y}$, The isotherm is belonging to type II and a very weak hysteresis loop

was observed indicating the loss in porosity nature because of filling the zeolite cavities by the complex. The BET surface area (S_{BET}) and total pore volume (V_p) were investigated and the computed values are given in Table 2. There is a drastic reduction of surface area and pore volume of zeolites upon introducing of the metal ion or its related complexes. Since the zeolite framework structure is not affected by encapsulation as shown from the XRD pattern, the reduction of surface area and pore volume provides direct evidence for the presence of complexes in the cavities and refers to the degree of filling the zeolite cavities⁽³⁷⁾. Specific surface areas (S_t) for all zeolites were estimated using V_{t-1} plots and are collected in Table 2. They are varying close to (S_{BET}), within the experimental error, indicating the correct choice of the reference t-curves.

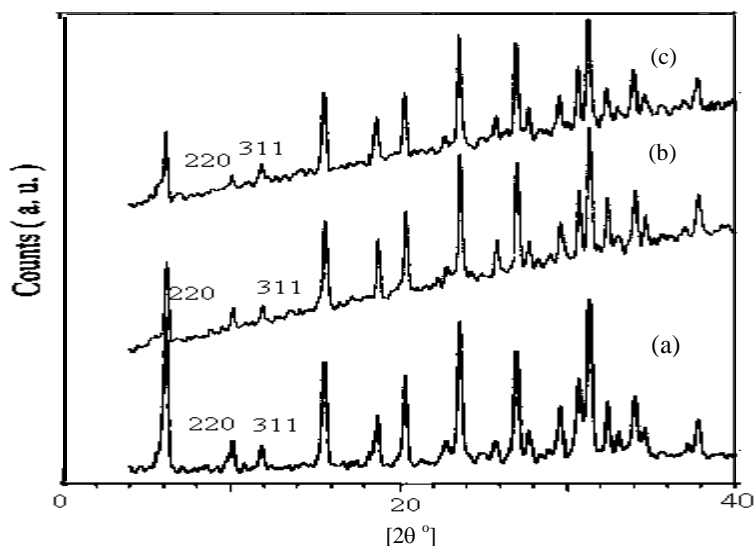


Fig. 2. X-ray powder diffraction patterns of (a) NaY, (b) Co^{II}-Y and (c) Co^{II}(SBSH)/Y.

Catalysis

CO-oxidation

Fig. 3 shows the FTIR spectra of the Co^{II}-Y and Co^{II}(SBSH)/Y catalysts after the adsorption of CO (equilibrium pressure of 50 Torr) at RT. Adsorption of CO on the catalysts led to the appearance of bands at [2350, 2197, 2167, 2118 (weak), 2044(weak)] and [2340, 2188(shoulder), 2159, 2112 and 2014] cm⁻¹ for Co^{II}-Y and Co^{II}(SBSH)/Y, respectively. It is clear that Co^{II}(SBSH)/Y showed the same group of bands like Co^{II}-Y. On the Co^{II}-Y sample (where Co ion are coordinated to several oxygens in the framework), the CO adsorption bands on Coⁿ⁺ ($n \leq 2$) sites has higher

frequency than that of Co^{II}(SBSH)/Y. Since coordination of cobalt sites with the hydrazone ligand (strong Lewis base) removes the Coⁿ⁺ ion from its position in the zeolite framework into the supercage and increases the electron density on Coⁿ⁺ (38,39).

Table 2. Surface area and pore volume data of NaY, Co^{II}-Y and Co^{II}(SBSH)/Y samples..

Sample label	S _{BET} (cm ² /g)	S _t (cm ² /g)	V _p (cm ³ /g)
NaY	873	860	0.80
Co ^{II} -Y	840	790	0.60
Co ^{II} (SBSH)/Y	519	577	0.49

Analysis of the FTIR results shows that the band near 2350 cm⁻¹ [Co^{II}-Y] / 2340 cm⁻¹ [Co^{II}(SBSH)/Y] developed during the CO adsorption on Co^{II}-Y and Co^{II}(SBSH)/Y has been attributed to the ν₃ vibration of physio-sorbed CO₂, linearly bound to the cobalt ions by ion-induced dipole interaction (40-42). The band 2350 cm⁻¹ [Co^{II}-Y] / 2340 cm⁻¹ [Co^{II}(SBSH)/Y] is an indication of CO₂ formation during the adsorption of CO on these catalysts. In fact, the oxidation of CO and formation of weakly bound CO₂ by CO adsorption on the catalysts are in agreement with the results reported elsewhere (40). The band at 2197 cm⁻¹ [Co^{II}-Y] / 2188 cm⁻¹ [Co^{II}(SBSH)/Y] is likely due to CO coordinated over surface Co²⁺ (in the β sites) whereas the band at 2167 cm⁻¹ [Co^{II}-Y] / 2159 cm⁻¹ [Co^{II}(SBSH)/Y] is assigned to Co²⁺-carbonyl (43-45). The two weak bands at 2118 cm⁻¹ [Co^{II}-Y] / 2112 cm⁻¹ [Co^{II}(SBSH)/Y] can be ascribed to Co-carbonyls containing cobalt in an oxidation state lower than two (44). So it is suggested that CO might reduce Co²⁺ to lower oxidation states. The evidence of different components in the IR absorption bands may be due to the existence of cobalt ions in different compositions and structures (46). All of the above mentioned peaks disappeared just after evacuation at room temperature indicating that, all CO and CO₂ might be evacuated or changed to another form (ca. other oxidation product). The spectrum of CO adsorbed at room temperature on Co^{II}-Y and Co^{II}(SBSH)/Y in the region of 1800-1650 cm⁻¹ (Fig. 4b, 5b) is dominated by a broad band at 1726 cm⁻¹ which is due to -COOH (47). By evacuation, the shoulder band observed at 1712 cm⁻¹ is assigned to νC=O of acids (48). It is clear that, some peaks might be assigned to carboxylate (-CO₂-) like species appear after evacuation at RT in both catalysts (Fig 4c, 5c). This may explain the disappearance of the Co-carbonyl species after evacuation at RT, i.e. CO oxidation occurred at the Co sites. By thermal evacuation at 50 °C, the bands

characteristic of $-\text{COOH}$ decreased in both catalysts (Fig. 4d, 5d) while the bands attributed to $-\text{C}=\text{O}$ (1712 cm^{-1}) and the carboxylate like species disappear in the $\text{Co}^{\text{II}}(\text{SBSH})/\text{Y}$ spectrum (Fig 5d) and still considerably detected in case of $\text{Co}^{\text{II}}\text{-Y}$ (Fig 4d). This may be due to the weak binding of these species onto Co sites in the $\text{Co}^{\text{II}}(\text{SBSH})/\text{Y}$ catalyst.

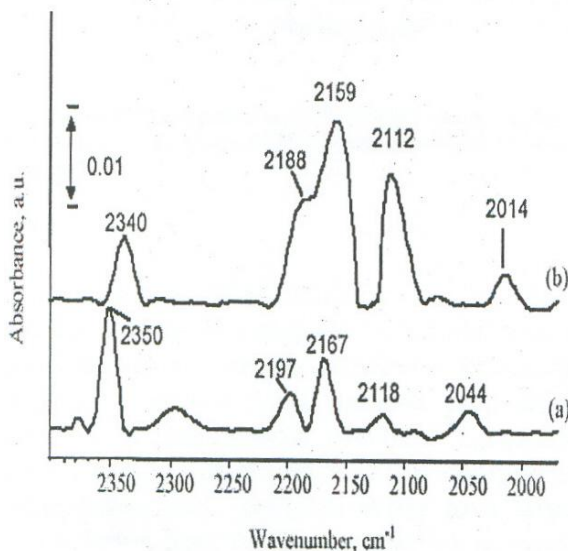


Fig. 3. The FTIR spectra of CO adsorbed on (a) $\text{Co}^{\text{II}}\text{-Y}$ and (b) $\text{Co}^{\text{II}}(\text{SBAB})/\text{Y}$ catalyst at room temperature (RT).

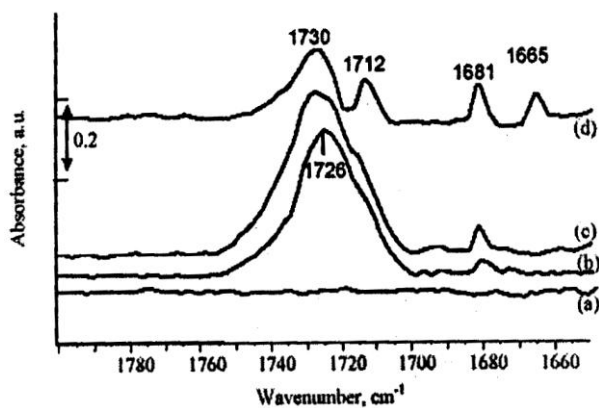


Fig. 4. The FTIR spectra of CO adsorbed on $\text{Co}^{\text{II}}\text{-Y}$ catalyst at the following conditions: (a) CO free catalyst, (b) after addition of 50 Torr of CO at room temperature, (c) evacuation at room temperature (RT) and (d) evacuation at 50°C .

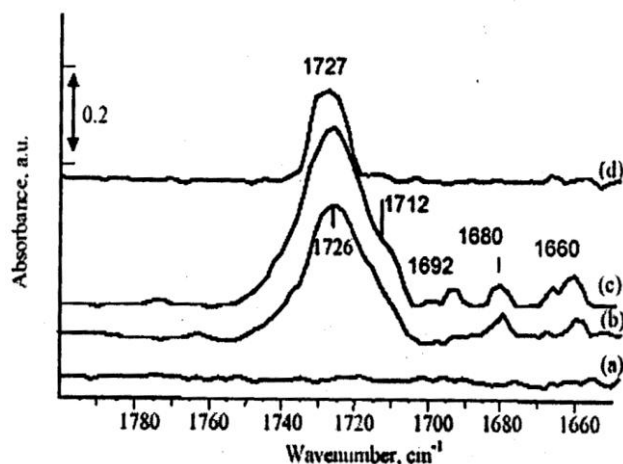


Fig. 5. The FTIR spectra of CO adsorbed on Co^{II}(SBSH)/Y catalyst at the following conditions: (a) CO free catalyst, (b) after addition of 50 Torr of CO at room temperature, (c) evacuation at room temperature (RT) and (d) evacuation at 50°C.

Conclusions

The results showed that Co^{II}(SBSH)/Y can be isolated by using FL method and Co(II) ions of the occluded complex coordinate to the hydrazone ligand to give 3:1 metal-ligand complex with an octahedral geometry. Although the reported results for a green Co(hydrazone) complex prepared in solution suggested a polymeric nature with a tetrahedral structure ⁽²⁹⁾, the different Physico-chemical studies on Co^{II}(SBSH)/Y disclosed that the composition and structure of the immobilized Co(hydrazone) complex differ to a large extent by encapsulation process. This deviation from the known solution chemistry was anticipated as the zeolite can exert an effect on the nuclearity of complexes. Thus we observed a trinuclear Co-L species inside the zeolite cages, where in solution the formation of polymeric structure is preferred. This suggested that the confinement of the complex inside the zeolite pores can prevent a polymerization due to the dimensions of the zeolite cage. The encapsulated complex is very stable up to 1000 °C inside Y zeolite assuming that the zeolite increases the thermal stability of the occluded complexes. Oxidation of CO forming CO₂ may be evidenced by the in-situ FT-IR spectroscopy and the data revealed that, the Co^{II}-Y and Co^{II}(SBSH)/Y are an active materials for CO adsorption / oxidation at room temperature and this may be considered as efficient alternatives for noble metal catalysts..

References

1. C. BOWERS AND P.K. DUTTA, *J. Catal.*, 122 (1990) 271.
2. N. HERRON, *Inorg. Chem.*, 25 (1988) 4714.
3. K. J. BALKUS Jr., A. A. Welch and B. E. Gnade, *Zeolites*, 10 (1990) 722.
4. S. KOWALAK, R. C. WEISS and K. J. Balkus Jr., *J. Chem. Soc., Chem. Comm.*, (1991) 57.
5. K. J. BALKUS JR., A. A. WELCH AND B. E. GNADE, *J. Incl. Phenom. Mol. Recogn. Chem.*, 10 (1991) 141.
6. A. G. GABRIELOV, A. N. ZAKHAROV, B. V. ROMANOVSKY, O. P. TKACHENKO, E. S. SHPIRO AND K. M. Minachev, *Koord. Chem.*, 14 (1988) 821.
7. G. MEYER, D. WHORLE, M. MOHL AND G. SCHULZ Ekloff, *Zeolites*, 4 (1984) 30.
8. K. J. BALKUS JR., S. KOWALAK, K. T. LY AND C.D. HARGIS, *Stud. Surf. Sci. catal.*, 69 (1991) 93.
9. K. J. BALKUS JR., C. D. HARGIS AND S. KOWALAK, *Am. Chem. Soc. Symp. Ser.*, 499 (1992) 347.
10. F. BEDIQUI, E. DE BOYSSON, J. DEVYNCK, K. J. BALKUS JR., *J. Chem Soc., Faraday Trans 87* (1991) 3831.
11. L. GALLION, N. SAJOT, F. BEDIQUI, J. DEVYNCK AND K. J. BALKUS Jr., *J. Electroanal. Chem.*, 345 (1993) 157.
12. R. F. PARTON, I. F. J. VANKELECOM, M. J. A. CASSELMAN, C. P. BEZOUKHANOUA, J. B. Uytterhoeven, P. A. Jacob, *Nature*, 370 (1994) 541.
13. N. HERRON, *J. Coord. Chem.*, 19 (1986) 25.
14. D. E. DE VOS, F. T. STARZYK, P. A. Jacob, *Angew Chem. Int. Engl.*, 33 (1994) 431.
15. N. HERRON, *Chem. Technol.*, 9 (1989) 542.
16. K. J. BALKUS Jr., A. G. Gabrielov and S. Bell, *Inorg. Chem.*, 33 (1994) 67.
17. F. BEDIQUI, L. ROUE, E. BRIOT, J. De vynck, S. Bell and K.J. Balkus Jr., *J. Electronanal. Chem.*, 373 (1994) 19
18. TRISSA JOSEPH, S. B. HALLIGUDI, C. SATYANARAYAN, DHANASHREE P. SAWANT, S. GOPINATHAN, *J. Mol. Catal. A : Chemical*, 168 (2001) 87.
19. EUGEN MOLLMANN, PETRA TOMLINSON AND W. F. HOLDERICH, *J. Mol. Catal. A: Chemical*, 206 (2003) 253.
20. K.MI ZUNO AND J.H. LUNSFORD, *Inorg. Chem.*, 22 (1983) 3484.
21. M. KOICHI, S. IMAMURA AND J. H. LUNSFORD, *Inorg. Chem.*, 23 (1984) 3510.

22. H. DIEGRUBER, P. J. PLATH AND G. SCHULZ - Ekloff, *J. Mol. Catal.*, 24 (1984) 115.
23. W. V. CRUZ, P.C.W. LEUNG AND K. SEFF, *J. Am. Chem. Soc.*, 100 (1978) 6997.
24. R. F. HOWE AND J. H. LUNSFORD, *J. Phys. Chem.*, 79 (1975) 1936.
25. T. A. O'BRIEN, K. ALBERT AND M.C. ZERNER, *J. Chem. Phys.*, 112 (2000) 3192.
26. M. A. VANNICE, IN: CATALYSIS, VOL. 3, EDS. J.R. ANDERSON AND M. BOUDART, Springer, Berlin (1982) p. 150, and references therein.
27. R. J. MADIX, *The Chemical Physics of Solid Surfaces and Heterogeneous Catalysis*, Vol. 4., Eds. D.A. King and D.P. Woodruff, Elsevier, Amsterdam, (1982) p. 1, and references therein.
28. R. D. KELLEY AND D. W. GOODMAN, *The Chemical Physics of Solid Surface and Heterogeneous Catalysis*, Vol. 4, Eds. D.A. King and D.P. Woodruff, Elsevier, Amsterdam (1982) p. 427, and references there in.
29. T. H. RAKHA, M. M. BEKHEIT AND K. M. IBRAHIM, *Transition Met. Chem.*, 17(1992) 517.
30. A. I. VOGEL, *A Text Book of Quantitative Inorganic Analysis*, Longmans, 5th Ed., London (1989).
31. W. G. EWING, *Instrumental Methods of Chemical Analysis*, 4th Ed., McGraw - Hill, Kogakusha (1975); A.I. Vogel, *A Text Book of Practical Organic Chem.*, 3rd Ed., Longman, (1975) p. 704.
32. A. B. P. LEVER AND D. OGDEN, *J. Chem. Soc.*, (1967) 2041.
33. A. B. P. LEVER, *Inorganic Electronic Spectroscopy*, Elsevier Publishing Company, Amsterdam (1968).
34. W. H. QUAYLE AND J. H. LUNSFORD, *Inorg. Chem.*, 21 (1982) 2226.
35. BRUNAUER, L. S. DEMING AND E. E. TELLER, *J. Am. Chem. Soc.*, 62 (1940) 1723.
36. K. S. W. SING, *Colloids and Surfaces*, Elsevier, Amsterdam, 38 (1989) 113.
37. K. J. BALKUS AND A. G. GABRIELOVE, *J. Incl.Phenom. Mol. Recognit. Chem.*, 21 (1995) 159.
38. H. HUANG, *J. Am. Chem. Soc.*, 95 (1973) 6636.
39. D. SCARANO, S. BORDIGA, C. LAMBERTI, G. SPOTO, G. RICCHIARDI, A. ZECCHINA AND C.O. AREAN, *Surf. Sci.*, 411 (1998) 272.
40. V. M. RAKIC, R. V. HERCIGONJA AND V. T. DONDUR, *Microporous Mater.*, 27 (1999) 27.
41. J. W. WARD AND H. W. HABGOOD, *J. Phys. Chem.*, 70 (1966) 1178.

42. P. A. JACOBS, F. H. CAUWELAERT, E. F. VANSANT AND J. B. UTTERHOVEN, J. Chem. Soc., Faraday Trans., 69 (1973) 1056.
43. D. B. AKOLEKAR AND S.K. BHARGAVA, Appl. Catal. A: General, 207 (2001) 355.
44. M. C. CAMPA, I. LUISETTO, D. PIETROGIACOMI AND V. INDOVINA, Appl. Catal. B: Environnemental, 46 (2003) 511.
45. A. A. KHASSIN, T. M. YURIEVA, V. V. KAICHEV, V. I. BUKHTIYAROV, A. A. BUDNEVA, E. A. PAUKSHTIS AND V. N. PARMON, Journal of Mol. Catal. A: Chemical, 175 (2001) 189.
46. E. FINOCCHIO ,T. MONTANARI, C. RESINI AND G. BUSCA, Journal of Mol. Catal. A: Chemical, 204(2003) 535.
47. K. KINOSHITA, Carbon, Electrochemical and Physical Properties, Wiley, New Yourk (1988), p. 87.
48. A.I. GRGOR'EV, N.V. DONCHENKO, A.M. DUNAEVA AND D.V. DEBABOV, Russ. J. Inorg. Chem., 30 (1985) 497.